Microwave Tomography: A Two-Dimensional Newton Iterative Scheme

Alexandre E. Souvorov, Alexander E. Bulyshev, Serguei Y. Semenov, Robert H. Svenson, Alexei G. Nazarov, Yuri E. Sizov, and George P. Tatsis

***Abstract*—In this paper, a variant of the Newton method, which uses a fast solution of the direct problem and a dual mesh, is proposed. Computational and physical experiments with simple two-dimensional high-contrast phantoms are discussed, and a full-scaled image of a two-dimensional mathematical model of a human torso is obtained.**

***Index Terms*— Image reconstruction, inverse problems, iterative methods, microwave imaging, Newton method, tomography.**

I. Introduction

MICROWAVE imaging of biological bodies has been of interest for a number of years [1]–[3]. Several two-dimensional tomographic systems have been reported to produce images of relatively simple phantoms and biological objects [1]–[5]. In our previous work [4], a two-dimensional prototype of a quasi-real-time microwave tomographic system with total acquisition time of approximately 500 ms was reported. This system was quick enough to obtain images of a living beating canine heart.

Spectral methods (based on so-called diffraction tomography (DT) [6]) prove to be very fast and capable of producing reconstructions with good quantitative accuracy for small contrast objects. However, if the first-order Born or Rytov approximation is not valid, the reconstructed images are seriously distorted. The iterative technique that combines DT and the direct-problem solution ([7] for the Born approximation and [8] and [9] for the Rytov approximation) considerably extends the useful working range of DT, but is still a subject of serious contrast limitations. More than a decade ago, several variations of the Newton procedure were introduced [10]–[12] that did not principally have contrast limitations. In spite of recent developments of this method [13]–[17], its applications are still limited to relatively small objects with dimensions of a few wavelengths. An accurate calculation of electric fields (needed by this method) requires a mesh discretization, which can describe the characteristics of the physical wave propagation. Estimations show that at least ten samples per wavelength are necessary to obtain an accurate solution [16]. For a frequency of 1–3 GHz, this sampling rate dictates a mesh with $N = 10^4$–10^5 elements per slice of human torso.

Manuscript received October 11, 1997; revised May 18, 1998.

A. E. Sourorov, A. E. Bulyshev, S. Y. Semenov, R. H. Svenson, and G. P. Tatsis are with the Laser and Applied Technologies Laboratory, Carolinas Medical Center, Charlotte, NC 28203 USA (e-mail: ssemenov@carolinas.org).

A. G. Nazarov and Y. E. Sizov are with the Kurchatov Institute of Atomic Energy, Moscow, Russia.

Publisher Item Identifier S 0018-9480(98)08025-9.

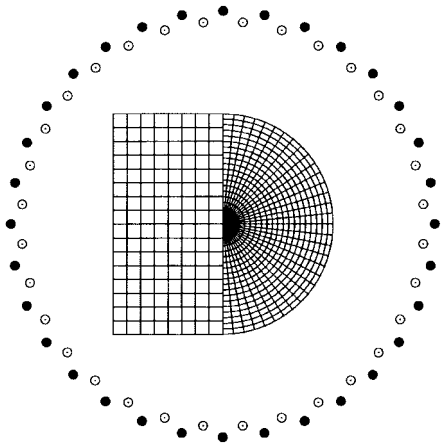

Fig. 1. Geometrical configuration of the problem. Solid circles: transmitters, hollow circles: receivers. The coarse Cartesian mesh is issued for the inverse problem, while the fine polar mesh is used for the direct problem.

To avoid sampling the electrical properties of the object with this extremely dense mesh, it seems natural to use a dual-mesh scheme first introduced in [16].

Since the number of operations per matrix inversion is proportional to N^3, with a mesh as large as this, the traditionally used method of the direct-problem solution by a discretization of the well-known Lipmann–Schwinger integral equation and the direct decomposition of the matrix turns out to be impractical. In [8] and [9], we have discussed a fast iterative solution of the direct problem. This method is very close to the algorithm proposed in [18]. Since the number of operations for it is mainly proportional to N, in this paper we are able to use a further modification of the algorithm in a Newton method for reconstruction of mathematical models of two-dimensional objects as large as a human torso.

The results of [13] show that the use of *a priori* information contributes to better and faster reconstructions. In this paper, we will show that in some cases the reconstruction by the Newton method is not possible without any *a priori* information.

II. Formulation

A. Newton Iterative Scheme

The geometry of the two-dimensional tomographic system is shown in Fig. 1. The transmitters and receivers are located around the object at finite discrete points. According to the standard perturbation theory [11], the change in the electrical

field registered by the jth receiver δE_{ij} due to a small change $\delta\varepsilon$ in the permittivity of the illuminated by the ith transmitter object is equal:

$$\delta E_{ij} = \frac{k_0^2}{\varepsilon_0}\int E_i(\mathbf{r})G_j(\mathbf{r})\delta\varepsilon(\mathbf{r})\,d\mathbf{r} = \hat{\mathbf{D}}\delta\varepsilon \tag{1}$$

where $k_0 = 2\pi\nu\sqrt{\varepsilon_0}/c$ and ε_0 are the wavenumber and permittivity in the immersion liquid, ν is the frequency, and c is the light velocity. The same wave equation with the point sources located at the corresponding transmitter and receiver points can be used for calculation of electrical field $E_i(\mathbf{r})$ generated in the object by the transmitter and Green's function $G_j(\mathbf{r})$ [11]

$$(\nabla^2 + k^2)E_i = -\delta(\mathbf{r} - \mathbf{r_i}) \tag{2}$$

$$(\nabla^2 + k^2)G_j = -\delta(\mathbf{r} - \mathbf{r_j}) \tag{3}$$

where $k = 2\pi\nu\sqrt{\varepsilon}/c$ is the wavenumber in the object and $\mathbf{r_i}$ and $\mathbf{r_j}$ are the coordinates of the transmitter and the receiver. Provided that $\hat{\mathbf{D}}$ is calculated, a step of the iteration procedure can be formulated as

$$\varepsilon^{n+1} = \varepsilon^n + \delta\varepsilon^n \tag{4}$$

$$(\hat{\mathbf{D}}^\dagger\hat{\mathbf{D}} + \alpha\hat{\mathbf{\Omega}})\delta\varepsilon^n = \beta\hat{\mathbf{D}}^\dagger(f^{\exp} - f^n) \tag{5}$$

where $\dagger$ signifies the conjugate transpose, and vectors $f^{\exp}$ and f^n denote the electrical field data E_{ij} measured in the tomograph and calculated with the current value of the permittivity ε^n. We use a standard Tikhonov regularization [19]

$$\hat{\mathbf{\Omega}} = -\nabla^2 = -\frac{\partial^2}{\partial x^2} - \frac{\partial^2}{\partial y^2} \tag{6}$$

with the regularization parameter α chosen empirically with a trial method. For the standard Newton iterations $\beta = 1$, but this process is known to diverge for extremely nonlinear problems. In this instance, it is helpful to slow down the iterations by choosing $\beta < 1$. Burov *et al.* [10] suggested to keep $\beta\|f^{\exp} - f^n\| < \|f^{\exp}\|$.

B. Direct Problem

In [8], we described a simple iterative method of the direct-problem solution. As long as the contrast between the immersion liquid and object is not too large, this method is very efficient. For example, in the case of water ($\varepsilon' = 80$) and myocardial tissue ($\varepsilon' = 54$), we need no more than 20 iterations to obtain a precision better than 10^{-4}. However, if the object includes such tissues as bones and fat, the iterations may diverge. In order to overcome this problem, we devised a more sophisticated version of the algorithm.

For definitiveness, let us consider (2). Introducing the incident wave $E_0 = -i\mathrm{H}_0^1(ik_0|\mathbf{r} - \mathbf{r}_i|)/4$, which is generated by the transmitter in the tomograph without an object, we can reformulate (2) in terms of the scattered wave $E_s = E_i - E_0$

$$(\nabla^2 + k^2)E_s = \left(k_0^2 - k^2\right)E_0. \tag{7}$$

Since the right-hand side of this equation is only nonzero inside the object, we can formulate absorbing boundary conditions on a circle of a radius R, which lies entirely beyond the boundaries of the object [8]. Namely, the Fourier transform of the scattered wave

$$\tilde{E}_s^m(r) = \int \exp(-im\varphi)E_s(r,\varphi)\,d\varphi \tag{8}$$

meet the following conditions:

$$\frac{\tilde{E}_s^m(R)'}{\tilde{E}_s^m(R)} = \frac{\mathrm{H}_m^1(k_0R)'}{\mathrm{H}_m^1(k_0R)} \tag{9}$$

where $\mathrm{H}_m^1(k_0R)$ is the Hankel function of order m.

In lossy media with $\varepsilon'' > 0$, the following nonstationary equation:

$$i\frac{\partial E_s}{\partial t} + (\nabla^2 + k^2)E_s = \left(k_0^2 - k^2\right)E_0 \tag{10}$$

will have the solution of (7) as its stationary limit, which can be found by using the implicit time iterations with the iteration parameter ξ

$$i\xi\left(E_s^{m+1} - E_s^m\right) + (\nabla^2 + k^2)E_s^{m+1} = \left(k_0^2 - k^2\right)E_0. \tag{11}$$

To solve this equation, we need a second loop of iterations

$$(i\xi + \nabla^2 + \bar{k}^2)E_s^{m+1,l+1} = (\bar{k}^2 - k^2)E_s^{m+1,l} + i\xi E_s^{m,l} + \left(k_0^2 - k^2\right)E_0. \tag{12}$$

Taking into account the boundary conditions (9), it is natural to solve (12) using the Fourier transform over the angle coordinate in the polar coordinate system. In this way, $\bar{k}$ can be a function of r. In our calculations, we try to minimize the norm of $\bar{k}^2 - k^2$ placing the value of $\bar{k}$ somewhere in the middle between the maximum and minimum of the k for a given r. The iteration parameter ξ plays an important role. In the limit of $\xi = 0$, (11) reduces to (7), and the whole process reduces to the iterations described in [8]. The smaller ξ is, the quicker the convergence of (11). In contrast to this, for small ξ, the process of (12) can slow down or even diverge, and the larger ξ is, the quicker the convergence of (12). In our calculations, we optimize this parameter so that every iteration of (12) at least halves the residual error (RE).

The number of iterations for this process does not depend on the mesh size. If the object and the immersion liquid have some absorption, a reasonable number of iterations provides the solution. In the worst case of the two-dimensional model of a human torso, 100 iterations were sufficient to obtain a precision about 10^{-4}.

Once the scattered field is calculated on the circle of a radius R, its values at the points of receivers can be obtained using the formula

$$\tilde{E}_s^m(|\mathbf{r}_i|) = \tilde{E}_s^m(R)\frac{\mathrm{H}_m^1(k_0|\mathbf{r}_i|)}{\mathrm{H}_m^1(k_0R)} \tag{13}$$

and the inverse Fourier transform.

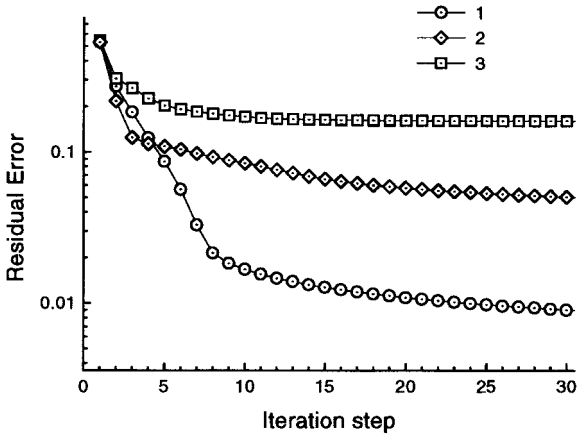

Fig. 2. Evolution of 1) noiseless data with *a priori* bounds on the complex permittivity, 2) noiseless data without bounds, and 3) noisy data (signal to noise ratio of 30%) with bounds.

C. Dual Mesh

With the above direct-problem-solution algorithm, we can afford a very fine mesh that is adequate to the physical properties of the wave propagating through the object as large as a human body. We use a uniform mesh in the polar coordinate system that can have as many as 512 nods over the angle and 200 nods over the radius. We cannot use the same mesh to describe the electrical properties of the object because we never have enough experimental data to reconstruct that many unknown values of the permittivity. Also, even if we did have them, the inversion of (5) would be a real computational burden. Fortunately, we never need a very large mesh to describe the electrical properties of the object [16]. For this purpose, we use a relatively coarse Cartesian mesh that can have up to 64 $\times$ 64 cells. The geometrical configuration of the problem is shown in Fig. 1.

III. Results

In order to test the above algorithm, we use a mathematical phantom that is composed of a cylinder of 8-cm diameter with two asymmetric segmental chambers and a small circular hole of a 1-cm diameter. The width of the wall between the chambers is 1.5 cm and the width of the outer wall varies in the interval of 1–1.5 cm. The walls of the phantom has $\varepsilon = 54 + i15$, while the immersion liquid, chambers, and holes have $\varepsilon = 80 + i10$. With the small hole playing the role of a damaged spot, it is not a big stretch to consider this phantom as a two-dimensional model of a heart that is immersed in water. With this mathematical phantom, we simulate measured data for the tomograph configuration, shown in Fig. 1, which is very close to our experimental device [4]. The tomograph has 32 transmitters located on a circle of 16.5-cm radius. For every transmitter, 16 receivers located behind the object on a circle of 16-cm radius receive the radiation. As we use a single frequency of 2.45 GHz, we have a set of 512 simulated measured data. We use a mesh of 512 $\times$ 200 cells in the calculation of the simulated measured data, which is more than adequate for obtaining a very high precision.

The initial value in all subsequent examples is the permittivity of the immersion liquid. The Cartesian mesh used in the inverse problem has 32 $\times$ 32 cells and the polar mesh for the direct problem has 128 $\times$ 64 cells. The evolution of the RE, which is the difference between the calculated electrical field and simulated measured data averaged over all transmitters and receivers, is shown in Fig. 2. The spatial scale in all figures is in centimeters.

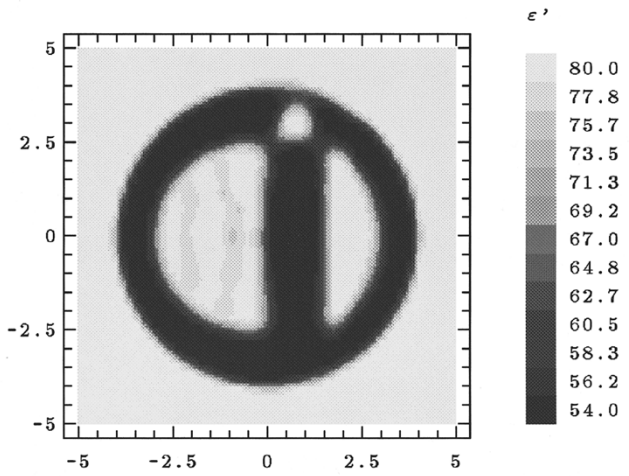

Fig. 3. Reconstructed image of the real part of the permittivity of the mathematical heart model. Noiseless data with *a priori* bounds.

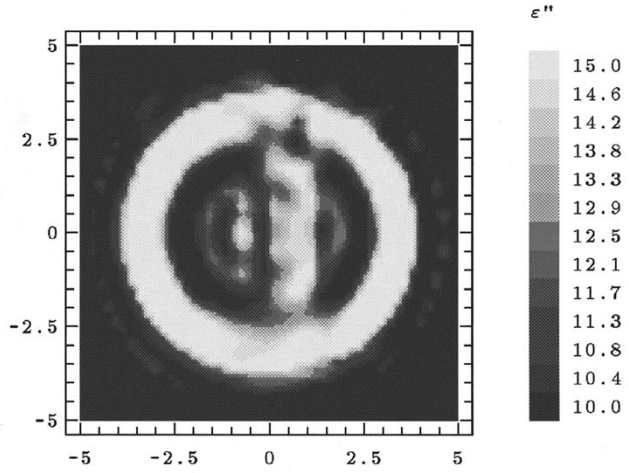

Fig. 4. Reconstructed image of the imaginary part of the permittivity of the mathematical heart model. Noiseless data with *a priori* bounds.

In our first example, we use the above reconstruction algorithm with *a priori* bounds on the maximum and minimum of the real and imaginary parts of the permittivity. The images of the real and imaginary parts of the permittivity obtained after 30 iterations are shown in Figs. 3 and 4, respectively. The quality of the real-part image is much better than that of the imaginary part because the contrast between the object and immersion liquid for the real part is more than for the imaginary part by a factor of approximately five. In our second example, we do not use any *a priori* information. In Fig. 2, we can see that the RE stabilized on a much higher level and the final image (see Fig. 5) is very far from the original. In the third example, we again use the *a priori* bounds with the

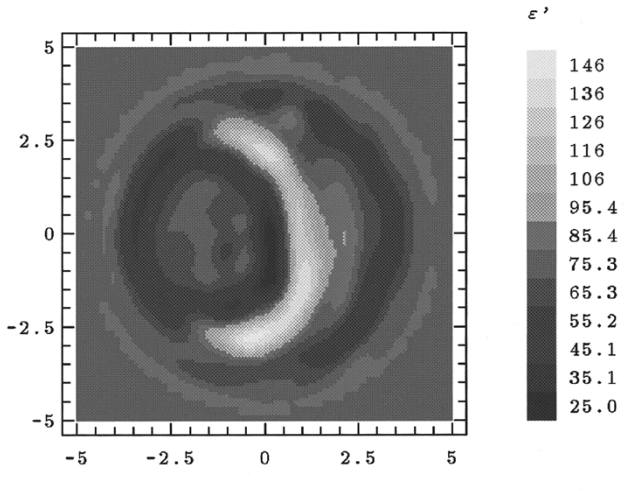

Fig. 5. Reconstructed image of the real part of the permittivity of the mathematical heart model. Noiseless data without *a priori* bounds.

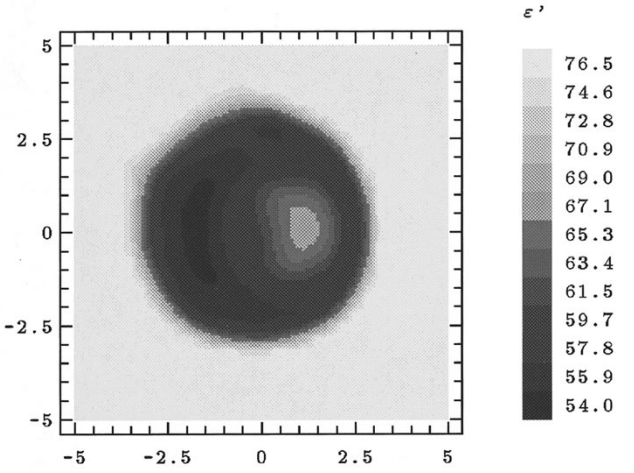

Fig. 7. Reconstructed image of the real part of the permittivity of the experimental phantom.

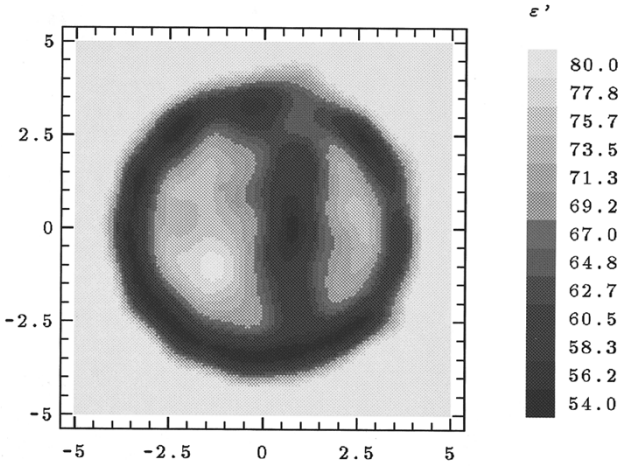

Fig. 6. Reconstructed image of the real part of the permittivity of the mathematical heart model. Noisy data (signal-to-noise ratio of 30%) with *a priori* bounds.

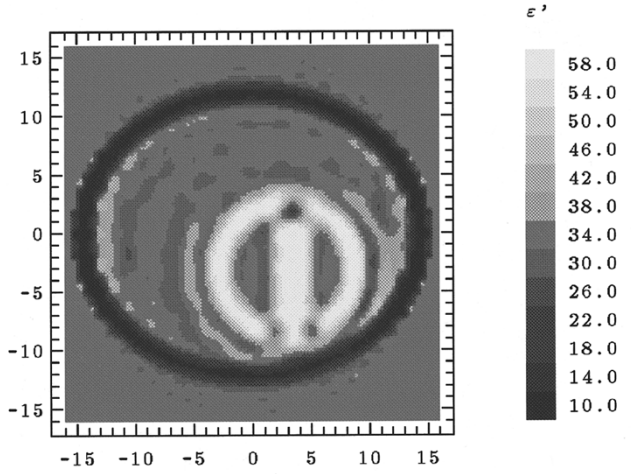

Fig. 8. Reconstructed image of the real part of the permittivity of the mathematical torso model. Noiseless data with *a priori* bounds.

simulated measured data with a signal-to-noise ratio of 30%. In this case, we need a much larger regularization parameter α and the RE is larger than even in the second example, but the image of the real part of the permittivity is still good enough (see Fig. 6).

For the experimental investigations, two asymmetrically enclosed cylindrical containers with thin plastic walls are used [8]. The container cylinders have diameters of 6.5 and 2.1 cm. The inner container is filled with water. The outer one is filled with a liquid with $\varepsilon = 54$. The phantom was placed in the center of the microwave chamber of our two-dimensional tomograph. The image in Fig. 7 is in very reasonable agreement with the real phantom.

To push our algorithm to its limits, we use a mathematical model of a torso with external dimensions 31 $\times$ 26 cm, which is composed of an elliptic 1.5-cm-thick shell with $\varepsilon = 10 + i2$. A model of the heart with a diameter of 13.5 cm and $\varepsilon = 58 + i21$ is placed inside the shell. The "heart" wall has three small holes of 1.5 and 2.5 cm. The immersion liquid, space inside the shell, heart chambers, and holes have $\varepsilon = 33 + i12$. The values of the permittivity are comparable to that of the involved biological tissues at the frequency of 1 GHz. A lower frequency is chosen because it offers a much better penetration depth and still reasonable resolution. The tomograph has 64 transmitters located on a circle of 30-cm radius. For every transmitter, 64 receivers located evenly on a circle of 20-cm radius receive the radiation. Thus, we have a set of 4096 simulated measured data. The image of the real part of the permittivity is shown in Fig. 8. All mentioned details of the torso (as well as some artifacts) can be clearly seen in this figure. In these calculations, we use a 64 $\times$ 64 Cartesian mesh and a 256 $\times$ 128 polar mesh.

All calculations were performed on a DEC Alpha-8200 computer.

IV. Discussion

In our previous report [8], we concluded that 32 receivers were not sufficient for imaging by the discussed spectral-

domain method. With the present spatial-domain method, we did not have such problems, and 32 receivers were adequate in our computational and physical experiments with relatively simple phantoms. Aside from this, this method proved to be more robust to noise contamination.

This paper, as well as other above-cited papers, illustrate that the Newton method is capable of finding the solution of very nonlinear problems. However, Fig. 5 shows that, in some cases, availability of *a priori* information can be very critical.

The proposed fast method of the direct-problem solution and a dual-mesh approach make it possible to use the Newton method for imaging two-dimensional objects with sizes and properties comparable to that of a human body. The last example proved to be a challenge for our DEC Alpha-8200 computer. The program had been running several hours before Fig. 8 was generated. Roughly speaking, in this case, the computational efforts were equal for the direct and inverse steps of the algorithm. There are still some possibility of further optimization of the direct-problem solution. The only reason we use the polar grid is that it naturally fits to the boundary conditions (9) and allows the fast Fourier transform. However, since this mesh has very small cells in the central region, some other mesh types with equally sized cells can cover the same surface with a smaller number of nodes. In this case, it may be possible to use the stationary equivalent of the approximate absorbing boundary conditions [20] in conjunction with some of the known methods of the elliptic equations solution (a very good short review of them may be found in [21]). Though the mesh of $64 \times 64 = 4096$ cells used for the inverse problem seems to be fairly sufficient in the two-dimensional case, this number is definitely very close to the upper limit. Taking into account the cubic dependence of the computational efforts to solve (5) by the direct decomposition, we can anticipate that further development of the Newton method will depend on the invention of a fast iterative solution of this equation. This is of particular importance for the three-dimensional case when we have to face a mesh that is at least 64 (and probably more) times larger.

REFERENCES

[1] L. E. Larsen and L. H. Jacobi, Eds., *Medical Applications of Microwave Imaging*. New York: IEEE Press, 1986.

[2] J. C. Bolomey and M. S. Hawley, *Methods of Hyperthermia Control*. Berlin, Germany: Springer-Verlag, 1990, ch. 2.

[3] M. Miyakawa and J.-C. Bolomey, Eds., *Non-Invasive Thermometry of the Human Body*. Boca Raton, FL: CRC Press, 1996.

[4] S. Y. Semenov, R. H. Svenson, A. E. Bulyshev, A. E. Souvorov, V. Y. Borisov, Y. E. Sizov, A. N. Starostin, K. R. Dezern, G. P. Tatsis, and V. Y. Baranov, "Microwave tomography: Two-dimensional system for biological imaging," *IEEE Trans. Biomed. Eng.*, vol. 43, pp. 869–877, Sept. 1996.

[5] P. M. Meaney, K. D. Paulsen, A. Hartov, and R. K. Crane, "An active microwave imaging system for reconstruction of 2-D electrical property distributions," *IEEE Trans. Biomed. Eng.*, vol. 42, pp. 1017–1026, 1995.

[6] A. J. Devaney, "A computer simulation study of diffraction tomography," *IEEE Trans. Biomed. Eng.*, vol. 30, pp. 377–386, July 1983.

[7] W. C. Chew and Y. M. Wang, "An iterative solution of two-dimensional electromagnetic inverse scattering problem," *Int. J. Imaging Syst. Technol.*, vol. 1, no. 1, pp. 100–108, 1989.

[8] S. Y. Semenov, A. E. Bulyshev, A. E. Souvorov, R. H. Svenson, Y. E. Sizov, V. Y. Borisov, V. G. Posukh, I. M. Kozlov, and G. P. Tatsis, "Microwave tomography. Theoretical and experimental investigation of the iteration reconstruction algorithm," *IEEE Trans. Microwave Theory Tech.*, vol. 46, pp. 133–141, Feb. 1998.

[9] S. Y. Semenov, A. E. Bulyshev, A. E. Souvorov, R. H. Svenson, Y. E. Sizov, I. M. Kozlov, V. Y. Borisov, V. G. Posukh, and G. P. Tatsis, "Two-dimensional microwave tomographic system," in *Proc. 18th Annu. Int. Conf. IEEE Eng. Medicine Biology Soc.*, Amsterdam, The Netherlands, Oct. 1996.

[10] A. Burov, A. Gorunov, A. Sascovez, and T. Tihonova, "Inverse scattering problems in acoustic," *Acoustic J.*, vol. 32, no. 4, pp. 433–449, 1986 (in Russian).

[11] W. C. Chew and Y. M. Wang, "Reconstruction of two-dimensional permittivity distribution using the distorted Born iterative method," *IEEE Trans. Med. Imag.*, vol. 9, pp. 218–225, Feb. 1990.

[12] N. Joachimowicz, C. Pichot, and J.-P. Hugonin, "Inverse scattering: An iterative numerical method for electromagnetic imaging," *IEEE Trans. Antennas Propagat.*, vol. 39, pp. 1742–1752, Dec. 1991.

[13] A. Franchois and C. Pichot, "Microwave imaging—Complex permittivity reconstruction with a Levenberg–Marquardt method," *IEEE Trans. Antennas Propagat.*, vol. 45, pp. 203–214, Feb. 1997.

[14] K. Belkebir, R. E. Kleinman, and C. Pichot, "Microwave imaging—Location and shape reconstruction from multifrequency scattering data," *IEEE Trans. Microwave Theory Tech.*, vol. 45, pp. 469–476, Apr. 1997.

[15] P. M. Meaney, K. D. Paulsen, and T. P. Ryan, "Two-dimensional hybrid element image reconstruction for TM illumination," *IEEE Trans. Antennas Propagat.*, vol. 43, pp. 239–247, Mar. 1995.

[16] K. D. Paulsen, P. M. Meaney, M. J. Moskowitz, and J. M. Sullivan Jr., "A dual mesh scheme for finite element based reconstruction algorithms," *IEEE Trans. Med. Imag.*, vol. 43, pp. 878–890, Sept. 1996.

[17] P. M. Meaney, K. D. Paulsen, A. Hartov, and R. K. Crane, "Microwave imaging for tissue assessment: Initial evaluation in multitarget tissue-equivalent phantoms," *IEEE Trans. Biomed. Eng.*, vol. 14, pp. 504–514, Mar. 1995.

[18] P. Concus and G. H. Golub, "Use of fast direct methods for the efficient numerical solution of nonseparable elliptic equations," *SIAM J. Numer. Anal.*, vol. 10, pp. 1103–1120, 1973.

[19] A. N. Tikhonov and V. Y. Arsenin, *Solutions of Ill-Posed Problems*. Washington, D.C.: V. H. Winston, 1977.

[20] G. Mur, "Absorbing boundary conditions for the finite-difference approximation of the time-domain electromagnetic-field equations," *IEEE Trans. Electromag. Compat.*, vol. 23, pp. 377–382, Apr. 1981.

[21] R. W. Hockney and J. W. Eastwood, *Computer Simulation Using Particles*. New York: McGraw-Hill, 1981, ch. 6.

Alexandre E. Souvorov was born in Novosibirsk, Russia, in 1953. He received the M.S. degree in physics from Novosibirsk State University, Novosibirsk, Russia, in 1975, and the Ph.D. degree in physics from Latvian University, Latvia, in 1979.

From 1975 to 1986, he was a Researcher at the Institute of Theoretical and Applied Mechanics, Novosibirsk, Russia. From 1986 to 1996, he was a Senior Researcher at the Institute of Heat and Mass Transfer, Minsk, Russia. He is currently a Research Scientist at the Carolinas Medical Center, Charlotte, NC. His research interest are inverse problems and transfer of radiation.

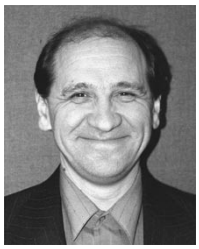

Alexander E. Bulyshev was born in Novosibirsk, Russia, in 1953. He received the M.S. degree in physics from Novosibirsk State University, Novosibirsk, Russia, in 1975, and Ph.D. degree in physics from Latvian University, Latvia, in 1979, and the professor in physics degree from Tomsk University, Russia in 1994.

From 1975 to 1996, he was a Researcher at the Institute of Theoretical and Applied Mechanics, Novosibirsk, Russia. He is currently a Research Scientist at the Carolinas Medical Center, Charlotte, NC. His research interest are inverse problems and transfer of radiation.

Serguei Y. Semenov was born in Moscow, Russia, in 1959. He received the M.S. degree in physics from Moscow State Lomonosov University, Moscow, Russia, in 1982, and the Ph.D. degree in biophysics and radiobiology from the Moscow Biophysical Institute, Moscow, Russia, in 1985.

Since 1988, he has been with the Kurchatov Institute of Atomic Energy, Russia. He is currently the Director of the Biophysical Laboratory, Kurchatov Institute of Atomic Energy, and also a Research Scientist at the Carolinas Medical Center, Charlotte, NC. His research interest are electromagnetic (EM) radiation interaction with biological tissues and nonionizing radiation tomography.

Robert H. Svenson received the B.A. degree from Lawrence University, Appleton, WI, in 1963, and the M.D. degree from the University of Chicago School of Medicine, Chicago, IL, in 1969.

In 1972, he completed his residency in internal medicine at the University of Chicago Hospitals and Clinics. He was a Post-Doctoral Fellow in the Division of Cardiology, Duke University Medical Center, Durham, NC. Since 1975 he has been a Cardiologist and Electrophysiologist at the Sanger Clinic, Charlotte, NC. In addition, he has served as the Medical Director of the Laser and Applied Technologies Laboratory, Carolinas Medical Center, Charlotte, NC. His research interests are cardiac physiology and electrophysiology.

Alexei G. Nazarov received the M.S. degree in radio physics and the Ph.D. degree in antennas and microwave technologies from the Moscow Power Engineering Institute (Technical University), Moscow, Russia, in 1992 and 1997, respectively.

He is currently with the Biophysics Research Laboratory, Kurchatov Institute of Atomic Energy, Moscow, Russia. His major research interests are system design and microwave equipment.

Yuri E. Sizov was born in Troitsk, Moscow Region, Russia, in 1961. He received the M.S. degree in electronic engineering from the Moscow Electronic Institute, Moscow, Russia, in 1984.

He is currently an Electronic Engineer in the Biophysical Laboratory, Kurchatov Institute of Atomic Energy, Moscow, Russia, and is an expert in electronic and computer engineering.

George P. Tatsis received the B.S. degree in biology from the University of North Carolina at Chapel Hill, in 1981, and the M.S. degree in biology from the University of North Carolina, Charlotte, in 1989.

From 1982 to 1988, he conducted cardiovascular research at the Heineman Medical Research Laboratories. Since 1988, he has served as the Administrative Director of the Laser and Applied Technologies Laboratory, Carolinas Medical Center, Charlotte, NC. In 1993, he also was appointed Director of Clinical Research of the Carolinas Heart Institute.